This document was prepared in conjunction with work accomplished under Contract No. DE-AC09-96SR18500 with the U.S. Department of Energy.

In-situ Monitoring of Corrosion during a Laboratory Simulation of Oxalic Acid Chemical Cleaning

B. J. Wiersma, J. I. Mickalonis, D. C. Beam, M. R. Poirier, D. T. Herman, S. D. Fink, J. M. Pareizs, and F. F. Fondeur

Savannah River National Laboratory
Aiken, SC, 29808

ABSTRACT

The Savannah River Site (SRS) will disperse or dissolve precipitated metal oxides as part of radioactive waste tank closure operations. Previously SRS used oxalic acid to accomplish this task. To better understand the conditions of oxalic acid cleaning of the carbon steel waste tanks, laboratory simulations of the process were conducted to determine the corrosion rate of carbon steel and the generation of gases such as hydrogen and carbon dioxide. Open circuit potential measurements, linear polarization measurements, and coupon immersion tests were performed in-situ to determine the corrosion behavior of carbon steel during the demonstration. Vapor samples were analyzed continuously to determine the constituents of the phase. The combined results from these measurements indicated that in aerated environments, such as the tank, that the corrosion rates are manageable for short contact times and will facilitate prediction and control of the hydrogen generation rate during operations.

Keywords: oxalic acid, carbon steel, hydrogen, radioactive waste tanks

INTRODUCTION

The Savannah River Site (SRS) will remove sludge as part of waste tank closure operations. Typically the bulk sludge is removed by mixing it with "water" to create a slurry and transporting the slurry to a downstream tank for processing. Experience shows that a residual heel may remain that cannot be removed by this conventional technique. In the past, SRS used oxalic acid solutions to disperse or dissolve the sludge heel to complete the waste removal. Since the waste tanks and cooling coils are constructed of carbon steel, a significant amount of corrosion may occur due to the acid. Although the total amount of corrosion may be insignificant for a short contact time, the corrosion reaction may generate a significant amount of hydrogen. One study indicates that with a 100 mpy (mils per year) corrosion rate, the lower flammability limit (LFL) will be reached in less than seven days (assuming no forced ventilation available). If such conditions exist, the project will need to develop and deploy costly safety class equipment modifications and procedures for the ventilation system.

To better understand the actual conditions generated by oxalic acid cleaning of carbon steel tanks, the authors developed and conducted an experimental program. As a starting point for that program, they

performed a literature review of the oxalic acid/carbon steel system. The prior studies included coupon and electrochemical tests. The tests used a variety of environmental conditions (e.g., de-aerated with argon or in air, and with temperatures from 25 to 95 °C). The common denominator in most of the tests was use of oxalic acid alone (i.e, no components from the dissolved sludge) and use of polished coupons (i.e., no mill-scale or corrosion products present). Most of those prior corrosion studies measured coupon degradation over a specific test period (e.g., 3 days, 6 days, or 2 weeks). Thus, it is not possible to discern if the corrosion rate changes with time during the planned processing. Because of passivation reactions that occur during corrosion of carbon steel in oxalic acid, and the changing environment due to dissolution of the sludge and due to agitation, application of the earlier corrosion data for the entire evolution may overestimate the actual corrosion rate and hydrogen generation rate for this specific process. The review also suggested that cathodic reactions other than hydrogen evolution might occur during the corrosion process. Other potential cathodic reactions include oxygen reduction or the reduction of another anion, such as nitrate, in solution. If either the corrosion rate decreases with time or the other cathodic reactions predominate, the hydrogen generation rate will be less and significant upgrades in the ventilation system may not be necessary.

The purpose of the experimental program was to investigate the chemical cleaning process to determine its effectiveness in dissolving sludge, the hydrogen generation rate, the generation rate of other gases, the carbon steel corrosion rate. The tests were conducted with simulated simulated sludge and tests in which simulated sludge was irradiated.

EXPERIMENTAL

Feed Preparation

To conduct the tests, personnel prepared supernate simulant, sludge simulant, and oxalic acid. The 8 wt.% oxalic acid solution was prepared with deionized (DI) water. A depleted uranium PUREX sludge simulant was prepared with composition shown in Table 1.
Experiments used a radioactive sludge containing DU as well as a non-radioactive sludge of the same approximate formulation that omitted the uranium. A second sludge stimulant was also prepared for the 50 °C experiment that investigated the influence of radiation. Table 2 shows that recipe.

Corrosion Coupon Preparation

The corrosion coupons used for these tests conform to the ASTM A537 Class I carbon steel (A537) specification. Table 3 shows the composition of this particular heat of steel.

The dimensions of each coupon were measured with digital calipers to the nearest 0.025 mm (or 0.001 inches). Typical dimensions for coupons used for the sludge dissolution and neutralization tests are 5 cm x 2 cm x 0.33 cm. The exception is the largest coupon (15 cm x 2 cm x 0.33 cm) that simulated the tank bottom during the sludge dissolution tests. Typical dimensions for coupons used for the hydrogen generation tests in presence of radiation are 2.23 cm x 1.27 cm x 0.33 cm. The coupons were weighed on an analytical balance to the nearest 0.0001 grams. Nominal initial weights for coupons for the sludge dissolution and neutralization tests ranged from 32 grams to 190 grams for the small and large coupons, respectively. The nominal initial weight for the coupons utilized for the (irradiated) hydrogen generation tests was 6 to 7 grams.

The initial surface condition of the coupons was a 600 grit polished finish (see Figure 1). The polished coupons provide a uniform, reproducible surface finish ideal for studying reactions between the steel and the environment. However, the metal surface conditions inside the tank are very different. Steel plates from the foundry, similar to those used to build the waste tanks, typically have an adherent iron oxide film on the surface referred to as mill scale. The presence of this film would be expected to produce a different corrosion response than the polished surface, at least initially.

To simulate the mill scale in these tests, coupons were placed in a Thermolyne™ benchtop muffle furnace set at 700 °C for 20 minutes. The result was a uniform oxide identified by x-ray diffraction as primarily magnetite (see Figure 1). Also, the tank steel has been exposed to caustic supernate for many years. To simulate this exposure, we immersed each coupon in simulated supernate for a minimum of 24 hours and then dried. This step left the coupon encrusted with a salt layer similar to the condition of the tank walls. Polished and mill scale coupons were employed for the sludge dissolution and neutralization tests, while only mill scale coupons were used for the hydrogen generation tests.

Equipment and Assembly for Sludge Dissolution Testing

To perform the corrosion measurements within each test vessel, an electrochemical cell was designed. The cell consisted of four primary features: a) a working electrode, b) a counter electrode, c) a reference electrode, and d) a potentiostat. Each feature is briefly described below.

The working, or corroding, electrode is the carbon steel coupon being tested. The coupons were prepared for testing by attaching a 22 AWG wire to one end of a coupon with silver epoxy. The coupon was then mounted in a chemically resistant acrylic compound to protect the exposed end of wire and the silver epoxy during the test and to provide an easily held sample. Multiple working electrodes were placed in each test vessel. Glass sample holders were designed to hold the coupons at specific locations and orientations. A single glass sample holder held the large coupon or "plate". This coupon was located at the bottom of the vessel such that the face was oriented parallel to the bottom of the vessel and the bottom side elevated by the glass holder to allow liquid contact on all edges. The small coupons were positioned in a "tree-like" holder with the face oriented approximately perpendicular to the bottom of the vessel (see Figure 2). Four to five small coupons were located at different heights in each vessel. For purposes of this report, the coupon holder positions are numbered 1 through 5 beginning with the lowest coupon. The wires from the coupons were extended through the top of the vessel via a glass tube, where they were then attached to the potentiostat.

In these tests carbon graphite rods served as the counter electrodes. Again, researchers attached a 22 AWG wire to one end of the rod with silver epoxy and covered with the acrylic mounting material. The rods were positioned to allow for a uniform current density to flow from the working electrodes (see Figure 2). Two rods were oriented vertically in the vessel such that the row of small coupons held by the tree-like holder was flanked on each side by a counter electrode. A single rod was oriented horizontally above the large coupon at the bottom of the vessel. The wires from the counter electrodes extended through the top of the vessel via the glass tube for connection to the potentiostat.

The reference electrode used in these tests was an ORION™ saturated silver/silver chloride (SSC) electrode. This electrode has shown excellent stability and reproducibility in previous high temperature testing with similar chemical systems. The reference electrode was held by a separate glass tube holder and fully immersed in the solution near the tree-like holder, away from the large sample (see Figure 3). The tests were performed with a PAR™ Model 273A Potentiostat/Galvanostat. The data acquisition software used for the PAR™ potentiostat was CorrWare™ for Windows.

Electrochemical Test Techniques for Sludge Dissolution Tests

The two electrochemical techniques performed during the sludge dissolution and neutralization tests were Corrosion Potential (E_{corr}) monitoring and Linear Polarization Resistance (LPR) [1]. Personnel monitored the corrosion potential of each working electrode to observe changes in the oxidizing or reducing conditions at specific locations in the vessel. Observing these changes assists in the determining the corrosion mechanism and whether or not hydrogen generation is thermodynamically possible.

Sludge Dissolution Simulation

Table 4 shows the conditions for the tests conducted. The inlet oxalic acid temperature was controlled to match the Dissolution Vessel temperature except in the highest temperature cases. In those experiments, the acid was maintained at 50 °C to minimize localized cooling when entering the vessel but to also avoid excessive evaporation over the 6 or 7 day duration[1] of the transfer.

Personnel conducted the simulated sludge chemical cleaning demonstrations as follows. They placed 7656 mL of 8 wt % oxalic acid in a glass vessel. They placed polypropylene beads on top of the oxalic acid and covered the vessel to minimize evaporation. They placed 190 g of simulated sludge containing depleted uranium into a ~ 22 L glass vessel. They added 775.6 g of simulated salt solution. The ratio of acid to sludge and the ratio of supernate to sludge mimic the values expected for the cleaning operations in the waste tank.

They then purged the vessel with air containing a helium tracer. The flow rates of helium and of air were 0.117 cm^3/min and 17 cm^3/min, respectively. The six demonstrations have an average vapor space turnover time of 853 min, which simulated the waste tank vapor space turnover rate. The volumetric turnover in the experiments was slightly lower than the nominal value and within the safety requirements for the tank. A slower turnover rate will increase the peak hydrogen concentration. Hence, the experiments are slightly conservative for peak hydrogen concentration relative to nominal operating conditions.

Once the oxalic acid and sludge reached the target temperatures, the oxalic acid was transferred to the sludge tank at ~ 0.7 mL/min. This rate was selected so the acid transfer occurred over approximately 7 days, similar to planned duration of oxalic acid transfer for the actual waste tank. Initially, the sludge tank mixer remained inactive to mimic the lack of mixing in the actual tank during the first acid additions until a sufficient liquid level is established to prime the pumps. In tests with mixing, the mixer was turned on after the liquid reached the agitator impeller. This point typically occurred after ~2 days, similar to the timing that may occur in full-scale operation. The mixing conditions – i.e., impeller dimensions and rotational speed – were selected to provide comparable mixing energy as expected during chemical cleaning operations with a circulating pump. Once the oxalic acid addition finished, the contact with sludge continued for ~50 hours.

The temperature of the acid-sludge slurry was monitored during the tests. The pH was measured daily with a pH probe or paper. The test sampled a portion of the off-gas stream using an online Agilent Model M300A Micro-GC gas chromatograph (GC) with a Molsieve 5A column for measurement of helium, hydrogen, oxygen, and nitrogen. Personnel added a PoraPlot Q column for measurement of carbon dioxide and nitrous oxide after Test 3. Argon was the carrier gas for the GC. Researchers used a gas standard of known composition to calibrate the peak areas prior to each test and to check the calibrations following each test.

Coupon Immersion Tests in an Irradiation Environment

These experiments measured the hydrogen generation rate due to corrosion of the carbon steel in an oxalic acid chemical cleaning solution mimicking tank chemical cleaning conditions. Previous testing focused on polished and pre-corroded specimen coupons in a de-aerated oxalic acid environment [2]. Researchers added sludge and supernate to the oxalic acid and mill scale samples (pre-treated with supernate). The experiments occurred in a radiation environment to simulate the effects of radiation on the hydrogen generation rate. Table 5 shows the test variables and matrix. The experimental design included replicates at each condition with and without radiation.

Equipment and Assembly

The coupon and test solution were situated inside a 45-mL stainless steel container (PARR™ Series 4700 Screw Cap Bomb). Each test occurred in a glass insert within the container to prevent the possibility of

galvanic corrosion between the coupon and the container. The containers were placed inside an aluminum block heated by band heaters. Type K thermocouples monitored container temperature and provided feedback to a temperature controller. The pressure in each container was measured with a Rosemount™ Model 1151DP pressure transducer. The transducers were calibrated with a range of 0 to 150 inches of water (0 to 5.4 psig). Approximately 8 to 10 feet of 1/8" stainless steel tubing connected the container to the sampling manifold. The sample manifold consisted of 1/8" and 1/16" stainless steel tubing. Sampling of the containers via the manifold was automated with a control system developed utilizing LabVIEW™ 7.1 (National Instruments). The control system actuated the solenoid valves (ASCO™ Series 8380) on the manifold.

Experiments occurred simultaneously in four test containers at a given test temperature. One of the aluminum blocks held two of the containers inside a radiation field. The radiation cell for these tests was a J.L. Sheperd Model 484™. The dose rate was set to 25,000 rad/hour to mimic the calculated dose rate from the remaining sludge in the actual waste tank. The pressure in the chambers was recorded by the software, so that the quantity of gas being produced was determined as a function of time. At a user selected frequency (typically 4 hours), or whenever the pressure in the chambers reached the maximum that can be measured by the instrumentation, a gas sample from one of the containers was collected.

Testing used two gas chromatographs (GC) for gas sample analysis. The primary GC for these tests was an Agilent 3000A Micro GC™ equipped with two columns to measure nitrogen, oxygen, hydrogen and carbon dioxide, with a MTI Model M200 Micro GC™ used as a back-up system. The latter model was capable of measuring only nitrogen, oxygen, and hydrogen. Personnel used a third GC to analyze several samples obtained manually. This GC was also an MTI Model M200, with the additional capability of analyzing for carbon dioxide and other components. The Agilent GC used the Cerity™ software, also developed by Agilent, to analyze the data, while the MTI Model M200 GCs used an older version of the EZChrom™ software developed by Agilent.

Post-test analyses and characterization

At the completion of the test, researchers removed the coupons from the test container for visual examination. During this examination, the form of corrosion on each coupon was identified (e.g., general) and differences in the corrosion products were noted. Photographs were taken to document the results. ASTM standard practices were followed to determine the general corrosion rate [3]. The corrosion products were removed from the sample by a two step process. First, loose corrosion products were removed using a wire brush. The coupons were then immersed in Clarke's solution (i.e., an inhibited HCl acid solution) to remove the final corrosion products. After removal of the corrosion products, the coupons were then weighed to determine the weight loss during the test. Solids collected at the bottom of the glass insert during the test. A few grams of these solids were collected and submitted for x-ray diffraction analysis for identification.

RESULTS AND DISCUSSION

Corrosion Results from Sludge Dissolution Tests

E_{corr} measurements

The results of the E_{corr} vs. time measurements for the six tests are shown in Figures 3 through 8. The time shown in each figure is relative to the initial addition of oxalic acid to the dissolution vessel. A line is drawn on each plot to indicate the potential below which hydrogen generation is possible based on thermodynamic considerations. Each figure shows the results from each coupon in the vessel. The "Plate" is the horizontal coupon at the bottom of the vessel. "Position 1" is the lowest vertically oriented coupon with the remaining vertical coupons identified consecutively as the distance above the vessel bottom increases.

The behavior of E_{corr} at the 50 and 75 °C was similar (see Figure 3, Figure 4, Figure 6 and Figure 7). At 50 °C and 75 °C, E_{corr} for the plate and Position 1 coupons initiated at potentials below E_{H2} and increased to potentials 150 to 200 mV greater than E_{H2}. The low initial E_{corr} was likely due to two factors: lack of mixing and surface condition. The lack of mixing left the metal in direct contact with oxalic acid for a period of time, rather than in contact with oxalic acid containing dissolved sludge. Visual observations of these two coupons during the test indicated that, at this stage of the test, the metal surface remained in a pristine (i.e., no iron oxides present) condition. Separate tests on pristine coupon in pure oxalic acid also resulted in E_{corr} values within this range. At these conditions, hydrogen evolution is the preferred cathodic reaction due to the limited amount of dissolved sludge present in the solution. The subsequent increase in potential is likely associated with the increase of ferric ion in solution as the sludge dissolves. Thus, the preferred cathodic reaction becomes ferric ion reduction. The E_{corr} for coupons in Positions 2 and 3, in contrast, initiated at values 100 to 200 mV greater than E_{H2} and remained at these values for the duration of the test. The higher E_{corr} values are likely due to the presence of sufficient ferric ion in solution which contacted the coupons initially.

The effect of mixing is also evident as shown in Figures 6 and 7. These tests yielded a greater difference in the values of E_{corr} than observed for the mixing tests. This result suggests that diffusion of the ferric ion limited the rate of the cathodic reaction. With mixing the concentration of the dissolved species remained more uniform and, thus, E_{corr} for all the coupons approached a similar value (see Figures 3 and 4).

The behavior at the lower temperature (25 °C) was also controlled by the cathodic reaction (see Figures 5 and 8). However, in this case the two competing reactions were oxygen reduction and hydrogen evolution. Unlike the higher temperature tests, we believe the concentration of ferric ion remained too low to affect the corrosion reaction. The effect of mixing is also apparent. In tests with mixing, shown in Figure 5, both the plate and position coupon were exposed to unmixed conditions for the first ~30 hours they were immersed – complete immersion of these coupons did not occur until 30 or 40 hours after oxalic acid addition began and mixing did not begin until after 70 hours. Initially, the potential for the plate coupon was less than E_{H2}. We believe sufficient sludge dissolution had occurred in the lower regions of the vessel to limit oxygen solubility near the plate coupon and thus hydrogen evolution was the favored cathodic reaction. However, the coupon in Position 1, behaved as though it were controlled by oxygen reduction initially. We believe this behavior occurred because at this point the sludge species had not yet diffused to the upper region of the solution. The availability of oxygen near the interface also favored the oxygen reduction reaction. As the species from the dissolved sludge solution diffused to the top of the liquid, E_{corr} for the coupon in Position 1 decayed as the solubility of oxygen decreased. At initiation of agitation, the plate and coupons in Positions 1 and 2 were immersed. The initial effect was that E_{corr} for all three coupons increased. This behavior indicates that oxygen reduction is a more significant participant in the cathodic reaction. However, after approximately 50 hours (i.e., the 120 hour mark of the test), E_{corr} for all three coupons began to decay to values below E_{H2}. We hypothesize the presence of other species from the dissolved sludge in the solution limited the availability of oxygen to these coupons. Thus hydrogen evolution became the controlling reaction. When the coupon in Position 3 became immersed approximately 90 hours after mixing initiated, the initial E_{corr} was less than E_{H2}. This trend suggests that the solution was saturated with species from the dissolved sludge at this time and thus the availability of oxygen was limited thereby hydrogen evolution became the preferred cathodic reaction at this location.

For the non-mixing test at low temperature, shown in Figure 8, E_{corr} for the plate and the coupon in Position 1 remained less than E_{H2} for most of the test. In contrast, E_{corr} for the coupons in Position 2 and 3 initiated at values 25 to 200 mV above E_{H2} and decayed slightly for the remainder of the test. It is speculated that a concentration gradient existed for the dissolved species in the sludge. The sludge dissolves at the bottom of the vessel and hence the concentration of dissolved species is greater at this location. The presence of these dissolved species in solution limits the availability of oxygen for the cathodic reaction. Thus, hydrogen evolution occurs at the plate and the coupon at Position 1. The concentration of the dissolved sludge species at the top of the liquid is less because these species have not yet diffused to this location. Thus, oxygen is more soluble and hence available to participate in the cathodic reaction at for coupons at Positions 2 and 3. The decay may reflect diffusion of the dissolved species toward the top of the liquid and hence a decreasing availability of oxygen.

The highest, or most noble, value of E_{corr} occurred during the 75 °C tests (see Figure 4). The E_{corr} for the horizontal plate shifted almost 250 mV after approximately 110 hours of exposure. These higher potentials typically indicate a shift into a passive region where corrosion rates are low. No such shift occurred in any other tests.

The Position 3 coupon tends to have the most positive or noble E_{corr}, while either the horizontal plate or Position 1 coupons have the most negative or active E_{corr} (see Table 6 and Figures 3 through 8). The higher values of E_{corr} were likely due to the increased presence of the ferric ion in solution that first contacts the coupon. The difference in E_{corr} between the Position 3 coupon and the horizontal plate coupon at any given time is a function of mixing. The difference in the potential is greater for the non-mixing cases. Both of these observations indicate that oxygen and the ferric ion are factors in the corrosion behavior.

Corrosion Rate Measurements

The corrosion rates also changed significantly during the experiments. Figure 9 shows an example of the changes. This figure shows the corrosion rate for the horizontal plate during Test 2 at 75 °C. Initially the corrosion rate is relatively low at approximately 5 mpy. Over the next 50 hours, the rate gradually increases to a maximum of 30 mpy. After 110 hours of exposure the corrosion rate decreases dramatically to less than 0.1 mpy. The drop in corrosion rate coincides with the positive shift in the E_{corr}. Heavy deposits were observed on the coupon at this time. Table characterizes similar shifts in corrosion rate for the other tests. Five characteristic corrosion rates are reported: 1) the initial corrosion rate (earlier than 2 hours), 2) the final steady state corrosion rate (reached after > 100 hours of exposure), 3) the corrosion rate while E_{corr} is less than E_{H2} (which provides an estimate of the rate of hydrogen generation), 4) the maximum corrosion rate at a given time, and 5) the time averaged corrosion rate. The latter corrosion rate is determined by integrating beneath the corrosion rate vs. time curve, and then dividing by the duration of the test. This corrosion rate is representative of the amount of damage the coupon experienced during the test and will be used as a realistic corrosion rate that may be applied to the tanks

The highest initial corrosion rates occurred on vertically oriented polished coupons at the highest temperatures. The highest corrosion rate reached 170 mpy on a Position 2 coupon during Test 2 at 75 °C. The lowest initial corrosion rates occurred on the mill scale coupons at any position. The presence of the mill scale is protective, at least initially, until the oxalic acid removes this layer.

The initial corrosion rates also demonstrate an effect of mixing. Test 3 with mixing and Test 6 without mixing occurred at 25 °C. The initial corrosion rate for the plate and Position 1 coupons are nearly identical for the two tests. During the initial stages of exposure for these coupons there was no mixing. However, the corrosion rates for the coupons in Positions 2 and 3 for the two tests are different by nearly two orders of magnitude. The higher corrosion rates during the mixing tests (Test 3) may be a result of increasing the availability of oxygen or ferric ion.

The corrosion rates passed through a maximum and then reach a steady state after greater than 100 hours of exposure. The highest steady state current density typically occurred on the Position 1 coupon. The lowest steady state current density typically occurred on the horizontal plate. These coupons are located next to each other and typically the values of E_{corr} were very similar. However, the top of the horizontal plate was typically covered with a thick layer of ferrous oxalate. The ferrous oxalate layer on the vertical coupon, in contrast, was typically disrupted resulting in areas with visible deep general corrosion and pitting.

In general, corrosion rates where E_{corr} was less than E_{H2} proved relatively low compared to the corrosion rates when E_{corr} was more positive. The highest observed corrosion rate for a situation with $E_{corr} < E_{H2}$ was 55 mpy on the Position 1 coupon during Test 3 at 25 °C. This rate occurred during the final few hours of the test when personnel increased the mixing speed in the vessel substantially. For the most part, corrosion rates when E_{corr} was less than E_{H2} remained less than 20 mpy.

The maximum instantaneous corrosion rates occurred typically between 50 and 100 hours of exposure on vertically oriented coupons, in the polished condition, while the solution was being mixed. The maximum rate observed was 170 mpy for the Position 2 coupon for Test 2 at 75 °C.

The corrosion rate for the horizontal plate during Test 2 at 75 °C decreased significantly after approximately 140. This decrease correlated with the increase in potential (-100 mV to +200 mV) observed on this coupon. This shift correlated with an active/passive transition observed in separate electrochemical tests [4]. The ferrous film that forms becomes more stable (i.e., lower corrosion rates) at these higher potentials. The figure also shows why caution is needed when extrapolating time-averaged corrosion rates to longer times. For example, if the test stopped after 192 hours, the time averaged corrosion rate would be 18 mpy. Although this estimate is not much greater than that measured (15 mpy), if the low corrosion rates observed after 192 hours continued to longer times, the corrosion rate would be overestimated. In contrast, an increasing corrosion rate at the conclusion of the test would result in the time-averaged corrosion rate underestimating the corrosion rate.

Table 7 contains the instantaneous hydrogen generation rates and the cumulative hydrogen generated for each coupon based on calculations from the corrosion measurements. The relationship between the corrosion rate and the hydrogen generation rate (G_r).

$$G_r = 3.8 \times 10^{-5} * CR * SA \qquad (1)$$

where CR is the corrosion rate in mpy and SA is the surface area of the coupon in ft^2. This equation is only applicable if the cathodic reaction that occurs is hydrogen evolution. The corrosion rates determined by the LPR measurements were used to estimate the rate at which hydrogen is evolving.

The instantaneous rates were obtained from the maximum corrosion rate, as measured by LPR, while E_{corr} was less than E_{H2}. The cumulative hydrogen evolved was calculated by integration of the instantaneous corrosion rate versus time plot. The time limits for the integration were defined by the time for which E_{corr} was less than E_{H2}. The predicted values exceed the values obtained from the GC measurements indicating a less than theoretical yield to hydrogen from the reactions.

The instantaneous generation rates from the coupons were similar for all the tests (typically 0.2-1 cm^3/hr) except for Test 4 (50 °C, unmixed), where the corrosion rate measured was extremely low. Hydrogen generation for the higher temperature tests tended to be during the initial stages when the coupon was first immersed. The mill-scale on the coupon may have provided initial protection and therefore a lower corrosion rate resulted.

Post-test Visual Examination of Coupons

The coupons appeared visually similar for all tests. The horizontal plate coupon from Test 2 at 75 °C (see Figure 10) is typical of the top surface of all the horizontal plates. Thick deposits of blue-green to yellow-green ferrous oxalate covered the surface. X-ray diffraction identified this layer as humboldtine (α-$FeC_2O_4 \bullet 2H_2O$), which is monoclinic ferrous oxalate and sodium ferrous oxalate, which is the orthorhombic ferrous oxalate ($Na_2Fe(C_2O_4)_2$), the dehydrated form of humboldtine [5]. Beneath this layer the surface was rough and uniformly corroded.

In contrast, both phases of ferrous oxalate deposits occurred randomly on the vertical coupons and on the bottom of the horizontal plate (see Figure 11). Between the ferrous oxalate deposits were regions covered by iron oxides, typically goethite or lepidocrocite. Although, the attack appeared uniform in most cases, isolated cases of pitting occurred on the vertical surfaces.

Coupon Immersion Tests in an Irradiation Field

These tests included direct measurement of the hydrogen generation rate during the corrosion experiment. The equipment monitored temporal pressure change in a closed vessel for a short period of time (i.e., 4 hours or less). The vessel was then vented to a gas chromatograph to measure the composition of the gas. The basic equation for determining hydrogen generation rate from these measurements is derived from the ideal gas law. The pressure, P, in the vessel is expressed as:

$$P = n\,R\,T/V \qquad (2)$$

where n is the number of moles, R is the gas constant (of 0.0821 mole-l/atm-K), T is the temperature in degrees K, and V is the volume in liters of the vessel, tubing and pressure transducer. For this test, T and V are constant and therefore the first derivative of equation 2 with respect to time is:

$$\frac{dP}{dt} = \frac{RT}{V} * \frac{d\Delta n}{dt} \qquad (3)$$

We assume that the primary gases generated from the corrosion process were hydrogen (designated as 1) and carbon dioxide (designated as 2). Therefore, the total moles of gas, n, is related to the mole fraction of gas that is measure by the gas chromatograph by:

$$\Delta n = n\,(x_1 + x_2) \quad (4)$$

where x_i is the mole fraction of the ith species. A constant, C, is defined as the ratio of x_2:x_1. Substitution of C into equation 3 gives:

$$\Delta n = n\,(1 + C)\,x_1 = (1 + C)\,n_1 \qquad (5)$$

Substitution of equation 5 into equation 3 and re-arrangement gives the following equation for the hydrogen generation rate:

$$\frac{dn_1}{dt} = (1+C)\,\frac{V}{RT}\,\frac{dP}{dt} \qquad (6)$$

The equation for carbon dioxide generation can then be related to the hydrogen generation rate by:

$$\frac{dn_2}{dt} = C\,\frac{dn_1}{dt} \qquad (7)$$

Thus by measuring the mole fraction of carbon dioxide and hydrogen, and the pressure change as a function of time, hydrogen generation and carbon dioxide rates can be calculated. The equation assumes that no other gases are generated. This assumption neglects the possibility of NO_x generation, which occurs due to the presence of nitrate in the supernate. Therefore, the hydrogen and carbon dioxide generation rates are likely overestimated initially. However, since there is a limited supply of nitrate in the supernate compared to the availability of the coupon and water, as the test proceeds this would become less of a factor.

Calculation of Gas Generation Rates

The hydrogen and carbon dioxide gas generation rates were calculated from equations 6 and 7. The maximum carbon dioxide generation rates during the initial stage ranged from 9×10^{-4} moles/hr to 3.5×10^{-3} moles/hour for the 50 °C and 75 °C tests, respectively. These rates were not impacted by exposure to the radiation source. Hydrogen generation rates during this time were negligible.

The highest hydrogen generation rates after this initial stage occurred in Container 3 for Test 1 at 50 °C (see Figure 12). In these tests, the hydrogen gas generation rate increased with time until the end of the

test. The maximum gas generation rate was approximately 5 x 10^{-5} moles/hour. A time averaged value of the gas generation rate was approximately 2.5 x 10^{-5} moles/hour for the irradiated tests and 1 x 10^{-5} moles/hour for the non-irradiated tests. The maximum hydrogen generation rate for the 75 °C test was approximately 7 x 10^{-6} moles/hour. A time averaged value of the hydrogen generation rate was approximately 2 x 10^{-6} moles/hour. It is interesting to note that the hydrogen generation rate did not appear to be influenced by radiation in this case. This rate also decreased with time to approximately 1 x 10^{-6} moles/hour. The hydrogen generation rates for the latter stages of the 25 °C tests were on the order of 1 x 10^{-8} moles/hour.

Hydrogen is also generated by radiolysis. Hydrogen generation by radiolysis may be estimated by:

$$D = G * D_{rad} * W * k \qquad (8)$$

where D is the gas generation rate in mL/h, G is the G-value total gas yield in molecules/100 ev, D_{rad} is the radiation dose in rad/h, W is the mass of the sample in g, and k is a temperature dependent combination of physical constants in (eV/g)(mL)/(rad-molecules). The dose rate for these tests was 25, 000 rad/h. The G-value is assumed to be 0.43 molecules/100 eV. The mass of the sample was approximately 20 g. The value for k ranged from 2.34 x 10^{-6} at 25 °C to 2.96 x 10^{-6} at 75 °C. The expected hydrogen generation rate due to radiolysis was calculated to be approximately 2.2 x 10^{-7} moles/hour at all the temperatures. This rate indicates that a relatively small fraction of the hydrogen that was generated during the 50 °C and 75 °C radiation tests (i.e., approximately 1% of the time averaged hydrogen generation rate for the 50 °C test and approximately 13% for the same at 75 °C). The hydrogen generation rate measured at the end of the 25 °C test is approximately one order of magnitude less than that expected from radiolysis. However, it is also recognized that the values for the gas generation rates were extremely low at this stage of the test and therefore might exaggerate experimental error.

The carbon dioxide generation rates in the latter stages of the tests remained relatively constant. The generation rates appeared to be a slight function of temperature. The highest rates occurred for the 75 °C tests (~ 1.2 x 10^{-5} moles/hour), while for the 50 and 25 °C tests showed lower rates (~8 x 10^{-6} moles/hour).

The observed generation rates indicate that corrosion plays a major role in the generation of hydrogen. Table 8 shows the estimated cumulative volume of hydrogen generated from corrosion assuming equation 1 is valid (i.e., hydrogen evolution is the cathodic reaction). The corrosion rates measured from weight loss measurements on the samples were utilized for this calculation. The table also shows the cumulative volume of hydrogen generated as calculated from the measurements of hydrogen generation rates (see equation 15). This value was calculated by integration of the instantaneous hydrogen generation rate curves. For the 50 °C test, the calculated cumulative volumes of hydrogen generated are in good agreement. This result indicates that corrosion was responsible for hydrogen evolution during this test. Thus it is likely that oxygen availability in the solution was limited and that an insignificant amount of ferric ion had dissolved into solution. The results from electrochemical tests with oxalic acid and Tank 8F sludge slurry suggest a similar interpretation.**Error! Bookmark not defined.**

For the 50 °C irradiated containers, the volume of hydrogen calculated from the hydrogen generation measurements is greater than that calculated from hydrogen evolution. The higher value is likely due to hydrogen evolved from radiolysis of the oxalic acid solution. Therefore, recombination of the hydrogen with oxygen in a gamma field does not appear to have occurred.

The agreement between the values for cumulative volume was not as good for 25 °C and 75 °C tests. In this case the volume calculated from the corrosion rate is significantly higher than that calculated from the hydrogen generation measurements. This difference indicates that another cathodic reaction was part of the corrosion mechanism. Both tests used sludge stimulant #1 and hence chemical composition does not account for the variance. In parallel electrochemical tests, it was observed that the presence of sludge simulant #1 in solution provided sufficient ferric ion to participate in the cathodic reaction. Initially hydrogen may have evolved due to de-aerated conditions in the container, however, once the sludge dissolved into the solution, ferric ion reduction became dominant.

Post-test Visual Examination of Coupons

The coupon and container contents were examined following the tests. Figure 13 is representative of the appearance of the coupons at all test conditions. The coupon was covered with a yellowish green precipitate. The amount of solids remaining on the specimen was approximately the same for each test. This precipitate could be removed by wire brush and subsequent cleaning with Clarke's solution. The precipitate was very difficult to remove from the coupons tested at 75 °C, which suggests a very tenacious film. A significant amount of yellowish green precipitate was suspended in the solution and observed at the bottom of the container. These solids were identified by x-ray diffraction as humboldtine. Interestingly, the solids contained no sodium ferrous oxalate, the orthorhombic structure. Given that the tests occurred in a dark environment, the photochemical reaction that forms this species was inactive. Therefore, carbon dioxide evolution during these tests was due to reactions within the sludge and radiolysis of the oxalic acid. No sludge solids were observed in the test container.

Once the precipitate was removed, the surface had a roughened appearance typical of general corrosion attack (see Figure 13). Some pitting of the surface was also observed.

Hydrogen Generation Measurements

Table 9 shows the gas generation during each of the tests. Since CO_2 productions accounts for most of the gas generated, we normalized the gas generation by the oxalic acid volume in the given test. After performing this normalization, the results agree within an order of magnitude.

Table 10 shows the hydrogen generation during each of the tests. Since the hydrogen is produced by a reaction between the oxalic acid and the sludge and by a reaction between the oxalic acid and the metal coupons, we normalized the hydrogen generation rates by each of these parameters. When normalizing by sludge mass, the actual waste and simulant tests results agree well. The radiation tests show larger volumes of gas being generated.

Based on the test results and scaling the hydrogen generation with metal surface area (8940 ft^2), we calculated the expected hydrogen generation rates in the waste tank as shown in Table 11 The hydrogen generation from the radiation tests does not agree well with that obtained from the other experiments, especially at 50 °C and 75 °C. The 50 °C radiation experiment used the Tank 8F washed sludge. Hence, the nitrate and nitrite scavengers are lower and one expects increased gas from radiolysis. However, this variance can not account for the marked increase in hydrogen observed. The most striking difference in test methodology for the radiation tests involved the use of a sealed system periodically purged with argon and then evacuated before backfilling with air. We speculate that the repeated evacuation led to thorough de-gassing of the liquid and removal of oxygen from the aqueous reaction. Under such anoxic conditions, passivating iron oxide films can not form and the reaction pathways change to enhance hydrogen generation. The post mortem analysis of the corrosion coupons for this experiment support this interpretation since iron oxides such as goethite ($HFeO_2$) and lepidocrocite (FeO(OH)) were not observed in these deposits. As such, we believe the radiation tests do not well mimic the planned operations and recommend not using this data for projecting to planned operations.

To assess this line of reasoning, we compared hydrogen generation rates measured previously in an anoxic environment compared to the tests performed in the cobalt source. The earlier tests exposed carbon steel in an 8 wt % oxalic acid solution at 50 °C that was de-aerated with argon. The tests used coupons covered with iron oxides. Table 12 compares the instantaneous corrosion rates after 1 week from the earlier tests with those measured from the present investigation. The table also shows the rate after two weeks from this study. After 1 week the hydrogen generation rates are within the same order of magnitude. The rates from the present studies are lower as expected given that the vessels were vented to the atmosphere and therefore exposed to oxygen periodically. During the second week of these studies, however, the irradiated containers were vented to the atmosphere on a less frequent basis, thus adding less available oxygen.

During the second week the hydrogen generation rate increased such that the difference between the two tests closed to within a factor of 2 to 6. This comparison suggests that conditions in the containers were approaching anoxic.

Additional studies were recommended to confirm this interpretation and to better comprehend the role of oxygen in this system. Analysis of the corrosion coupons from the actual waste demonstration could provide additional confirmation of the presence of protective oxide films during the planned cleaning process and confirmation of similar analyses from the demonstrations with simulated waste. Also, additional experiments – simplified in nature – to explicitly study the role of oxygen on the reactions and to quantify the oxygen transfer rates in these slurries would enhance process understanding.

Since most of the gas generated in the process demonstrations and actual waste experiments was carbon dioxide and the carbon dioxide is produced in reactions with oxalate, we scaled the gas generation with oxalic acid. Based upon the test results and the expected operating conditions in the waste tank (100,000 gallons oxalic acid), we calculate the gas generation during chemical cleaning shown in Table 13.

Table 13 shows the maximum hydrogen generation rate measured during each of the simulant demonstrations. At 50 °C and 75 °C (mixed), no hydrogen was detected, so the corresponding generation rate is calculated based on the hydrogen in the gas being equal to the minimum concentration of hydrogen measured during the corresponding unmixed test. The table shows the maximum generation calculated with no correction, with the helium correction, and with the nitrogen correction. The table also shows the generation rate normalized by carbon steel coupon surface area, and the maximum hydrogen generation rate in Tank 5F based on the surface area of carbon steel (8940 ft^3).

CONCLUSIONS

In the past, SRS used oxalic acid solutions to disperse or dissolve the sludge heel to complete the waste removal. To better understand the actual conditions of oxalic acid cleaning of carbon steel tanks, an experimental program was conducted to determine the hydrogen generation rate, the generation rate of other gases, and the carbon steel corrosion rate.

Measured corrosion rates for the process demonstrations using simulated sludge #1 depended primarily on temperature, agitation and orientation of the coupon. For tests with agitation of the solution, the maximum time-averaged corrosion rates measured 40 mpy, 30 mpy and 86 mpy for the 25, 50 and 75 °C tests, respectively. For tests without agitation, the maximum time-averaged corrosion rates decreased to 11 mpy, 0.76 mpy, and 36 mpy for the 25, 50 and 75 °C tests, respectively. The corrosion rate for the 50 °C non-agitated test appears inexplicably low. As a conservative estimate for this case a bounding value of 24 mpy was assumed by calculating the average of the corrosion rates at 25 °C and 75 °C.

Testing used horizontal coupons to simulate the tank bottom and the maximum time-averaged corrosion rates on these coupons proved lower than for the tank walls (i.e., vertical coupons). For tests with agitation, the corrosion rates measured 0.5 mpy, 5 mpy and 15 mpy for the 25, 50 and 75 °C tests, respectively. For the tests without agitation, the corrosion rates were 0.87 mpy, 0.23 mpy, and 0.49 mpy for the 25, 50 and 75 °C test, respectively.

The maximum time-averaged corrosion rates tests in the presence of radiation were 15 mpy, 60 mpy, and 12 mpy for the 25, 50 and 75 °C tests, respectively. Three differences between these corrosion rates and those measured in the process demonstrations are noteworthy. The sludge simulant for the 50 °C test differed from that used for the simulant demonstrations. Secondly, although the irradiated test container was aerated initially, we believe that the liquid became de-aerated with time, whereas ventilation settings in the process demonstrations (mimicking planned operating conditions) replenished the oxygen content of the liquid. Third, the tests with radiation continued for 15-20 days versus 10 days for the demonstrations. The longer time may have resulted in either higher or lower corrosion rates than observed during the process simulations.

Based on the experimental results from the process demonstrations with simulated and actual waste, and scaling the hydrogen generation with metal surface area (8940 ft^2), the expected total hydrogen generation (for a single nominal 10-day cleaning cycle – experiments ranged from 9-14 days) in the waste tank for the proposed cleaning process follows. The highest instantaneous generation rate from these experiments, projected to tank conditions, equates to 0.03 ft^3/min.

In the process demonstrations and in the actual waste tests, the gas composition was dominated by carbon dioxide formed from the corrosion reactions. Tests also showed presence of nitrous oxide (as high as 3.3 vol %), about an order of magnitude less than the carbon dioxide. Analyses did not reveal the presence of any other flammable or combustible gases that pose process concerns.The highest instantaneous total gas generation rate from these experiments, projected to tank conditions, equates to 655 ft^3/min.

The irradiated tests generated markedly more hydrogen, but comparable total gas, at the higher temperatures (i.e., 50 °C and 75 °C) than observed in the other experiments. This behavior also occurred in the controls for those experiments, indicating radiation itself did not cause the elevated hydrogen. The irradiation test method included pulling vacuum on the sample containers and we believe this approach de-gassed the liquid removing oxygen. The absence of oxygen prevented formation of protective oxide solids observed in other experiments as confirmed by x-ray diffraction of coupons. Since the process demonstrations with simulant involved comparable mixing energies and ventilation conditions as the planned operations, the authors select these results as representative of planned operations.

REFERENCES

1. "Standard Test Method for Conducting Potentiodynamic Polarization Resistance Measurements," ASTM G59-97, Re-approved in 2003.
2. H. D. Smith, R. L. Russell, and G. K. Patello, "Evaluation of Hydrogen Gas Generation from Oxalic Acid Contact with the Carbon Steel of a High Level Waste Storage Tank," In Environmental Issues and Waste Management Technologies in the Ceramic and Nuclear Industries, Eds. J. C. Marra and G. T. Chandler, Ceramic Transactions, Vol. 93, pp. 221-227, 1999.
3. "Standard Practice for Laboratory Immersion Corrosion Testing of Metals," ASTM G31-72, Reapproved in 1999.
4. B. J. Wiersma and J. I. Mickalonis, "Electrochemical Studies on the Corrosion of Carbon Steel in Oxalic Acid Cleaning Solutions", Corrosion 2008, Paper No. 1675.
5. R. M. Cornell and P. W. Schindler, Clays and Clay Minerals, Vol. 35, No. 5, 347-352, 1987.

Table 1. Simulated sludge #1 target composition (based on equilibrium calculations).

Component	wt %	Component	wt %
$Al(OH)_3$	11.30	$Ni(OH)_2$	10.02
$BaSO_4$	0.52	$Pr(OH)_3$	0.15
$CaCO_3$	2.36	$SrCO_3$	0.06
CaF_2	0.14	$UO_2(OH)_2$	17.31
$Ca_3(PO_4)_2$		Ag_2CO_3	0.21
$Cr(OH)_3$		$Ba_3(PO_4)_2$	
$Fe(OH)_3$	44.50	$Ca(OH)_2$	1.37
HgO	0.15	$CePO_4{\cdot}2H_2O$	0.19
$KMnO_4$		$Pu(OH)_4$	0.02
$La(OH)_3$	0.15	$Sr_5(PO_4)_3OH$	0.12
$Mg(OH)_2$	0.37	$ZnCr_2O_4$	0.59
$Mn(OH)_2$	10.01	ZrO_2	0.49

Table 2. Sludge stimulant #2 used in 50 °C radiation tests

Cations	wt %, dry		Anions	wt %, dry
Aluminum, Al	9.59		Carbonate, CO_3^{2-}	5.13
Calcium, Ca	2.11		Nitrite, NO_2^-	5.87
Copper, Cu	0.13		Nitrate, NO_3^-	1.95
Iron, Fe	24.34		Total Hydroxide, OH^-	24.7
Potassium, K	0.005		Oxide, O^{2-}	11.4
Magnesium, Mg	0.12		Phosphate, PO_4^{3-}	0.13
Manganese, Mn	2.73		Sulfate, SO_4^{2-}	0.64
Sodium, Na	7.20			
Nickel, Ni	2.79			
Silicon, Si	0.76		**Specific Gravity**	1.1
Strontium, Sr	0.09			
Zinc, Zn	0.27		**Total Solids, wt %**	16.0

Table 3. Material test report for ASTM A537 Class I carbon steel. The compositions shown are in wt %.

Al	C	Cr	Cu	Mn	Mo	Ni	P	S	Si	Fe
0.066	0.18	0.16	0.157	1.31	0.055	0.18	0.018	0.01	0.279	balance

Table 4. Test matrix for process demonstrations with simulated waste.

Test	Dissolution Vessel Temperature (°C)	Oxalic Acid Temperature (°C)	Mixing
1	50	50	Yes
2	75	50	Yes
3	25	25	Yes
4	50	25	No
5	75	25	No
6	25	25	No

Table 5. Test matrix for hydrogen generation tests in radiation field.

Test	Temperature (°C)	Sludge	Gamma Radiation	Test Duration (hours)
1	50	Simulated Tank 8F (no U)	Yes	405
2	50	Simulated Tank 8F (no U)	No	405
3	75	Simulated Tank 5F (no U)	Yes	330
4	75	Simulated Tank 5F (no U)	No	330
5	25	Simulated Tank 5F (no U)	Yes	476
6	25	Simulated Tank 5F (no U)	No	476

Table 6. Corrosion results for coupons from Dissolution Vessel.

Test	Coupon Position	E_{corr} at time < 2 hours (mV)	Final Steady State E_{corr} (mV)	Time that E is less than E_{H2} (hours)	Corrosion Rate at time < 2 hours (mpy)	Final Steady State Corrosion Rate (mpy)	Corrosion Rate while E < E_{H2} (mpy)	Maximum Instantaneous Corrosion Rate (mpy)	Time Averaged Corrosion Rate (mpy)
1 (50°C, polished, mix)	Plate	-331	-135	< 10	3.4	9	3.4	10	5
	1	-395	-112	< 60	7.7	74	7.7	78	30
	2	-80	-125	0	3.5	52	NA	66	28
2 (75°C, polished, mix)	Plate	-359	+198	72	3.5	0.1	3.5	30	15
	1	-356	-78	< 2	24	85	24	128	67
	2	-147	-91	0	70	70	NA	170	86
3 (25°C, mill-scale, mix)	Plate	-264	-300	146	0.02	0.4	0.02-0.65	0.65	0.5
	1	-26	-287	237	6	55	1-55	55	15
	2	-211	-293	160	3	30	3-30	30	21
	3	-300	-310	78	20	50	20-50	50	40
4 (50°C, mill-scale, no mix)	Plate	-425	-40	82	0.32	0.2	0.22-0.32	0.32	0.23
	1	-471	-55	100	0.7	0.7	0.74-0.81	0.81	0.76
	2	139	-60	0	0.55	0.5	NA	1.25	0.34
	3	-116	-165	0	0.15	0.3	NA	0.36	0.28
5 (75°C, mill-scale, no mix)	Plate	1	-70	0	0.2	0.25	NA	1.3	0.45
	1	-407	-130	23	8	16	6.2-25.8	70	36
	2	6	40	0	0.45	0.6	NA	0.77	0.49
	3	217	240	0	0.07	0.08	NA	0.1	0.08
6 (25°C, mill-scale, no mix)	Plate	84	-315	197	0.05	0.44	0.05-1.9	1.9	0.87
	1	-369	-310	171	6	18	6.3-30.1	30.1	11
	2	-38	-180	0	0.02	0.02	NA	0.02	0.02
	3	-244	-204	< 7	0.002	0.003	0.0024	0.0024	0.002

Table 7. Estimated hydrogen generation rates based on the corrosion rate measurements during the process demonstrations.

Test	Coupon Position	Surface Area (ft^2)	Time $E_{corr} < E_{H2}$ (hours)	Maximum Corrosion Rate while $E_{corr} < E_{H2}$ (mpy)	Maximum Instantaneous Hydrogen Generation Rate (cm^3/hour)	Predicted Cumulative Hydrogen Generated (cm^3)
1	Plate	0.18	10	3.4	0.61	4.9
	1	0.02	60	7.7	0.16	6.6
2	Plate	0.18	72	3.5	0.69	20
	1	0.02	2	24	0.51	11
3	Plate	0.18	146	0.65	0.097	57.7
	1	0.02	237	55	1.03	59.7
	2	0.02	160	30	0.56	65.1
	3	0.02	78	50	0.93	12.2
4	Plate	0.18	82	0.32	0.053	4.4
	1	0.02	100	0.81	0.027	1.6
5	1	0.02	23	25.8	0.57	8.1
6	Plate	0.18	197	1.9	0.32	40
	1	0.02	171	30	0.56	31
	3	0.02	7	0.0024	< 0.0025	< 1

Table 8. Estimation of hydrogen generation from corrosion rate measurements.

Test	Container	Surface Area (ft^2)	Corrosion Rate from weight loss measurements (mpy)	Cumulative Hydrogen Generated as Calculated by equation 2 (cc^3)	Cumulative Hydrogen Generated as Calculated from the Hydrogen Generation Rate Measurements (cc^3)
1	1 (irradiated)	0.0083	37.6	129	170
	2	0.0085	29.7	104	105
	3 (irradiated)	0.0081	59.6	193	252
	4	0.0084	21.4	73	60
2	1 (irradiated)	0.0084	10.7	32	14
	2	0.0083	12.9	39	25
	3 (irradiated)	0.0078	10.6	29	11
	4	0.0080	12.1	35	9
3	1 (irradiated)	0.0043	9.8	19	0.03
	2	0.0086	15.9	48	NA
	3 (irradiated)	0.0081	9.1	33	0.04
	4	0.0043	12.3	30	0.0002

Table 9. Gas generation during chemical cleaning tests.

Test	Purge Gas (cm^3)	Gas Generation He correction (cm^3)	Gas Generation N_2 correction (cm^3)	Gas Volume Generated per unit volume Oxalic Acid
Simulant: 50 °C, mixed	416,000	-36,000	55,000	7.2
Simulant: 75 °C, mixed	246,000	82,000	87,000	11.4
Simulant: 25 °C, mixed	339,000	21,000	26,000	3.4
Simulant: 50 °C, unmixed	345,000	115,000	109,000	14.2
Simulant: 75 °C, unmixed	229,000	119,000	79,000	10.3
Simulant: 25 °C, unmixed	248,000	13,000	26,000	3.4
Radiation 50 °C	N/A	N/A	218-288	14.5 – 19.2
Radiation 75 °C	N/A	N/A	170 - 192	9.4 – 10.7
Radiation 25 °C	N/A	N/A	103 - 189	5.7 – 10.5

Table 10. Hydrogen generation during chemical cleaning tests.

Test	Purge Gas (cm^3)	H_2 Generation N_2 correction (cm^3)	H_2 Generation corrected for sludge (ft^3/kg)	H_2 Generation corrected for metal surface area (ft^3/ft^2)
Simulant – 50 °C mixed	216,000	1.2	0.00023	0.00018
Simulant – 75 °C mixed	246,000	1.8	0.00033	0.00028
Simulant – 25 °C mixed	339,000	1.5	0.00028	0.0.00023
Simulant – 50 °C unmixed	345,000	6.2	0.00120	0.00100
Simulant – 75 °C unmixed	229,000	2.7	0.00050	0.00040
Simulant – 25 °C unmixed	229,000	3.3	0.00061	0.00051
Radiation – 50 °C	N/A	170 - 253	40 - 60	0.72 – 1.07
Radiation – 75 °C	N/A	11 - 14	1.9 – 2.5	0.047 – 0.059
Radiation – 25 °C	N/A	0.03 – 0.04	0.0053 – 0.0071	0.00013 – 0.00017

Table 11. Projected hydrogen generation in waste tank based on experiments.

Temperature (°C)	Hydrogen generation (ft^3 ±100%)	
	Mixed	Unmixed
Process Demonstrations		
25	1.7	4.6
50	<1.6*	8.9
75	<2.5*	3.6
Actual Waste Experiments		
50	0.6	
75	0.15	
Radiation Tests		
25		1.5
50		9600
75		530

* based on detection limit for on-line gas analyses

Table 12. Comparison of hydrogen generation rates in an anoxic environment with rates determined from the radiation tests.

Test	Hydrogen Generation Rate after 1 Week (moles/h)	Hydrogen Generation Rate after 1 Week (moles/h)
Average of two tests in an Anoxic Environment	7.7×10^{-5}	-
Average of Vessels 1 and 3 from this investigation.	1.6×10^{-5}	3.9×10^{-5}
Average of Vessels 2 and 4 from this investigation.	7.0×10^{-6}	1.2×10^{-5}

Table 13. Projected total gas generation in Tank 5F based on experiments.

Temperature (°C)	Gas generation (ft^3 ±10%) Mixed	Unmixed
Process Demonstrations		
25	45,000	45,000
50	96,000	189,000
75	152,000	138,000
Actual Waste Experiments		
50	184,000	
75	28,000	
Radiation Tests		
25		140,000
50		257,000
75		143,000

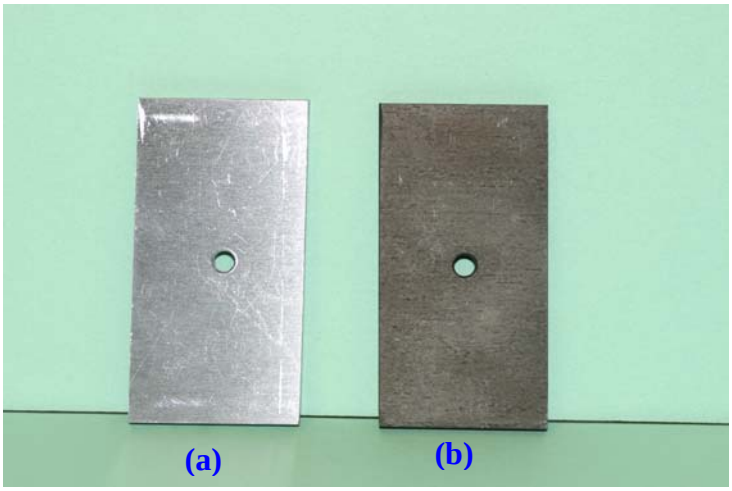

Figure 1. Typical coupons for process demonstrations: a) polished coupon and b) mill scale coupon.

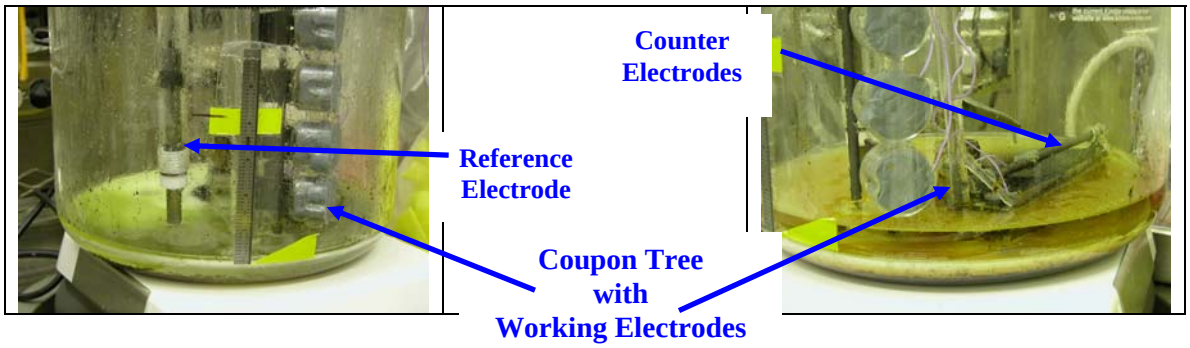

Figure 2. Photograph showing the relative location of the electrodes in the vessel.

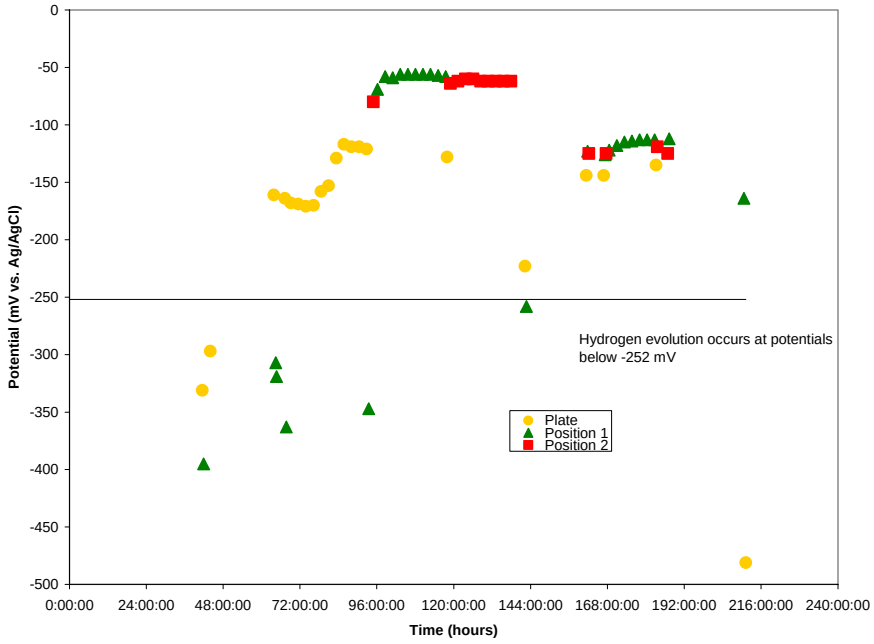

Figure 3. E_{corr} measurements for Test 1 (mixed at 50 °C): polished coupons.

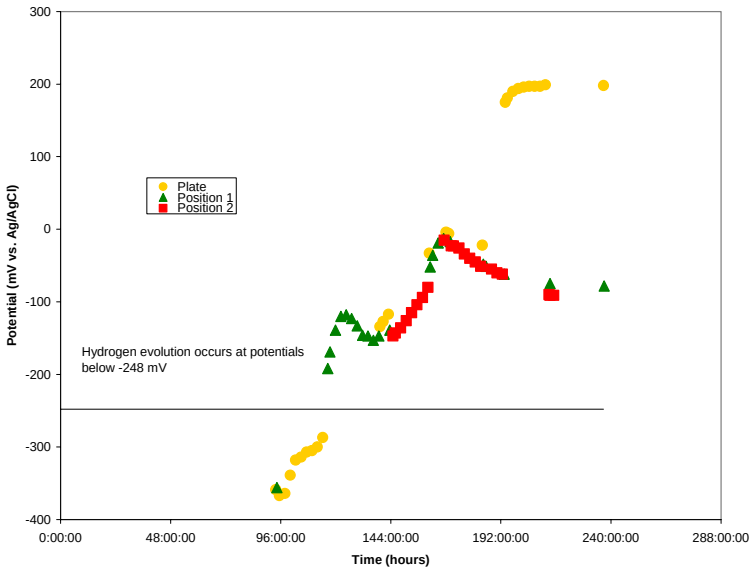

Figure 4. E_{corr} measurements for Test 2 (mixed at 75 °C): polished coupons.

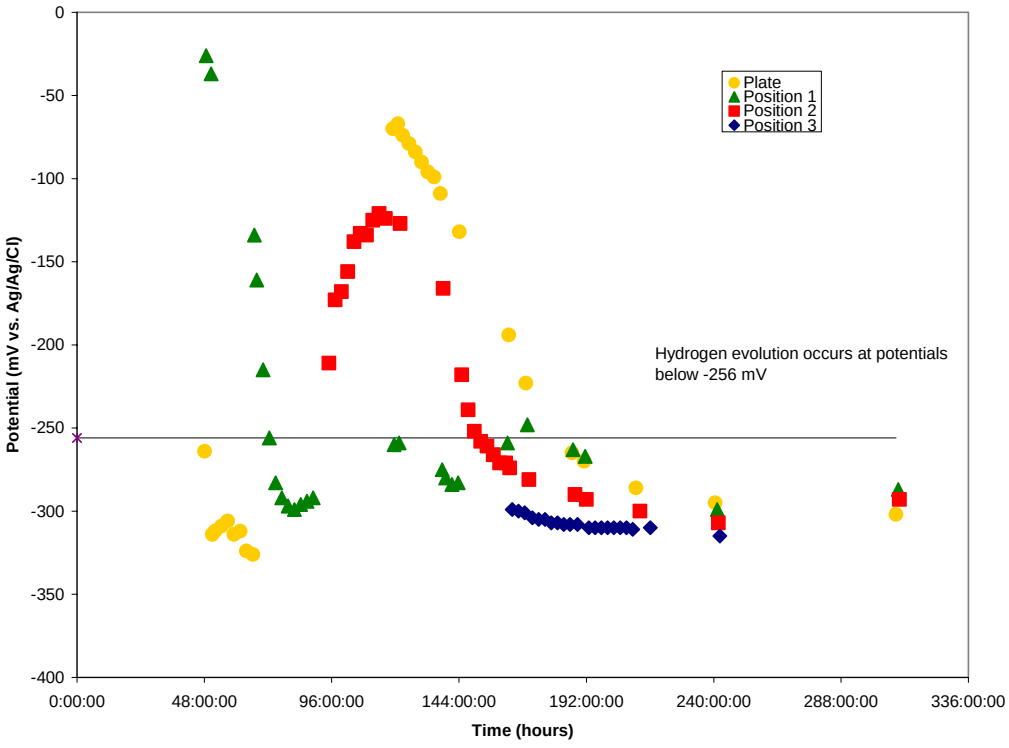

Figure 5. E_{corr} measurements for Test 3 (mixed at 25 °C): mill-scale coupons.

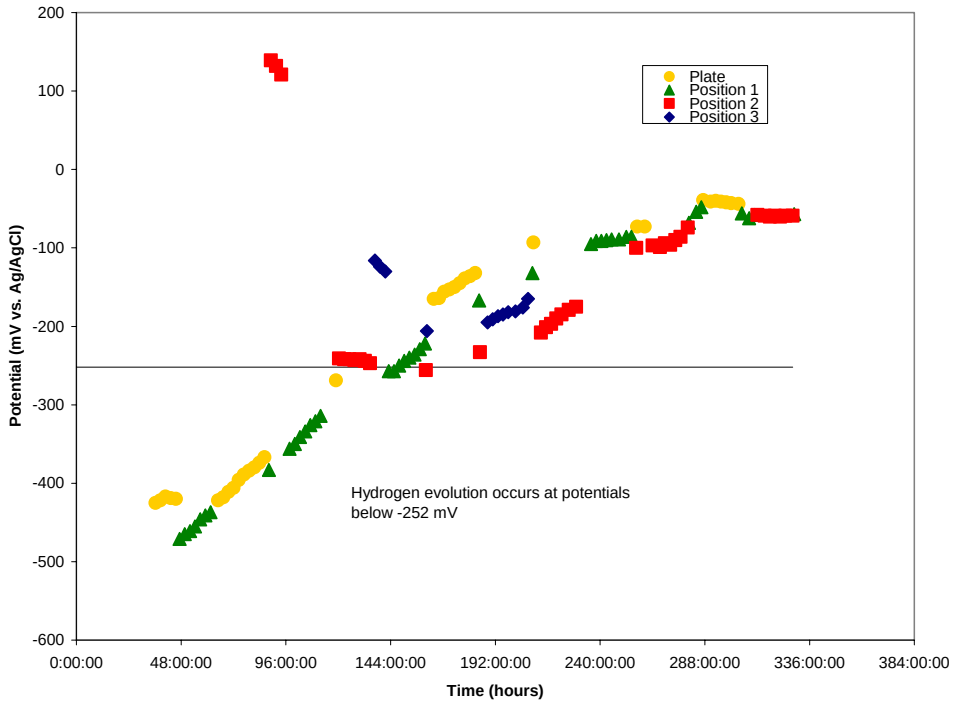

Figure 6. E_{corr} measurements for Test 4 (unmixed at 50 °C): mill-scale coupons.

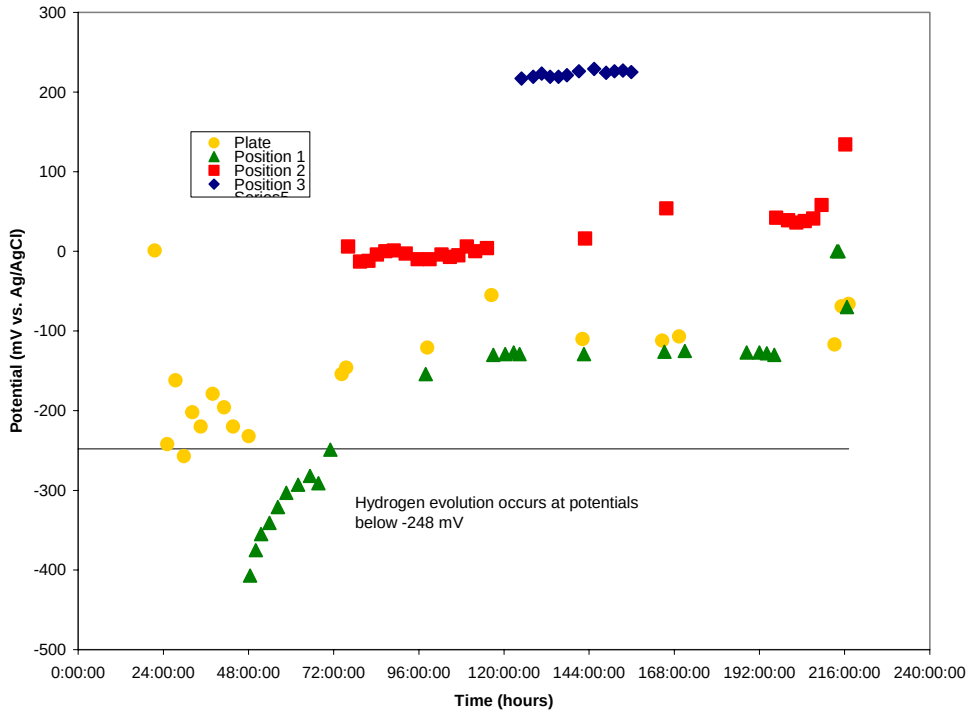

Figure 7. E_{corr} measurements for Test 5 (unmixed at 75 °C): mill-scale coupons.

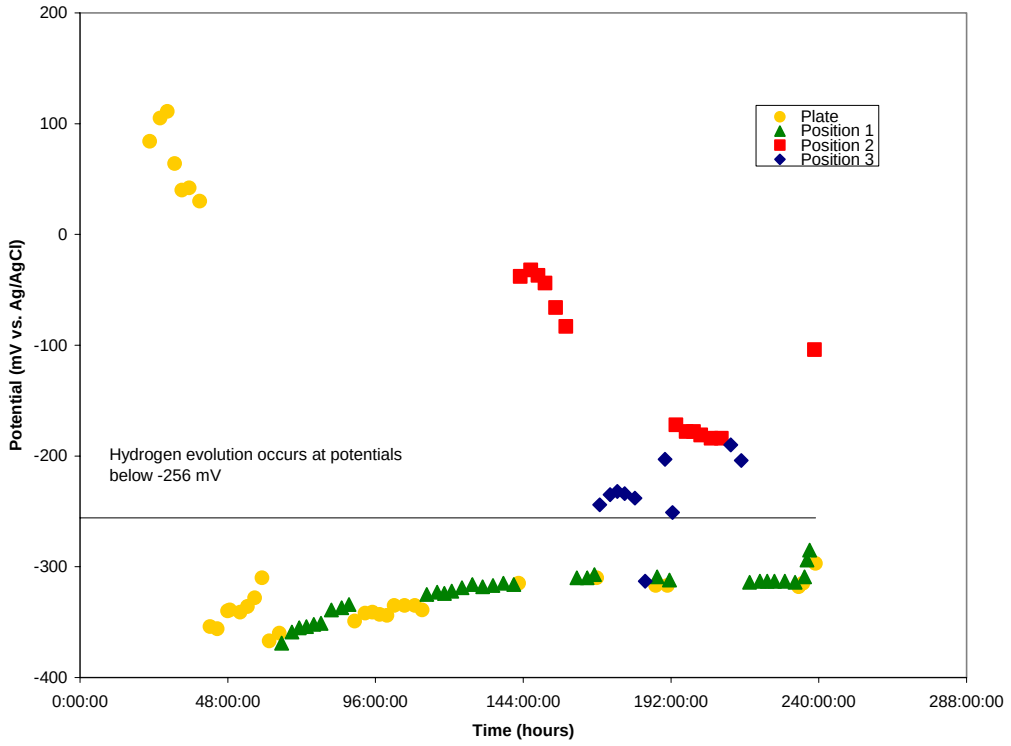

Figure 8. E_{corr} measurements for Test 6 (unmixed at 25 °C): mill-scale coupons.

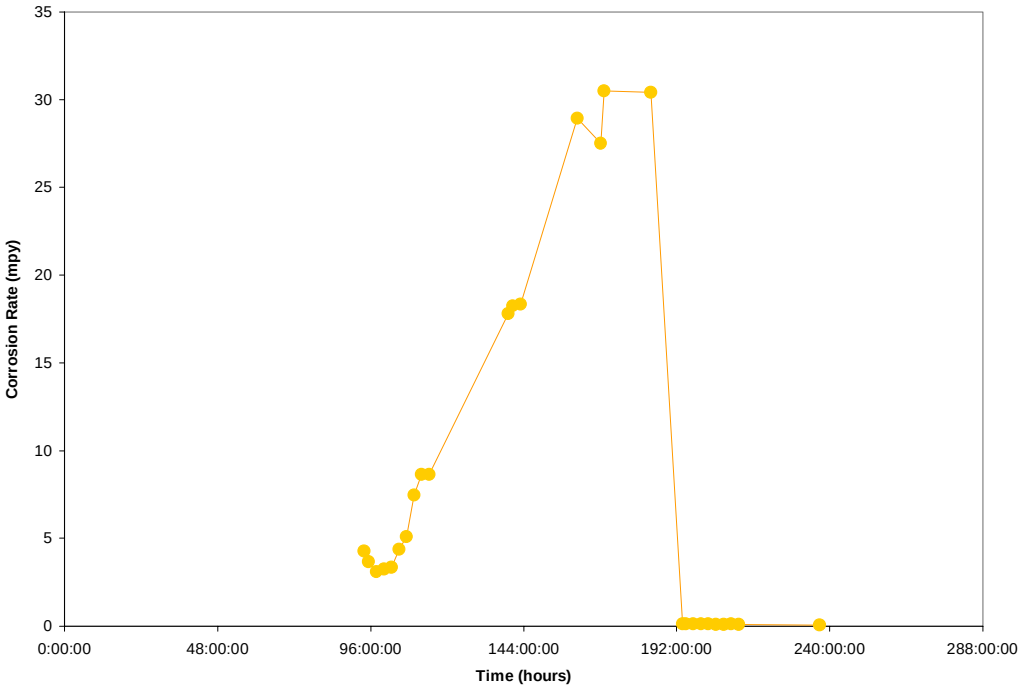

Figure 9. Corrosion rate as a function of time for the horizontal plate during Test 2 (75 °C, mixed).

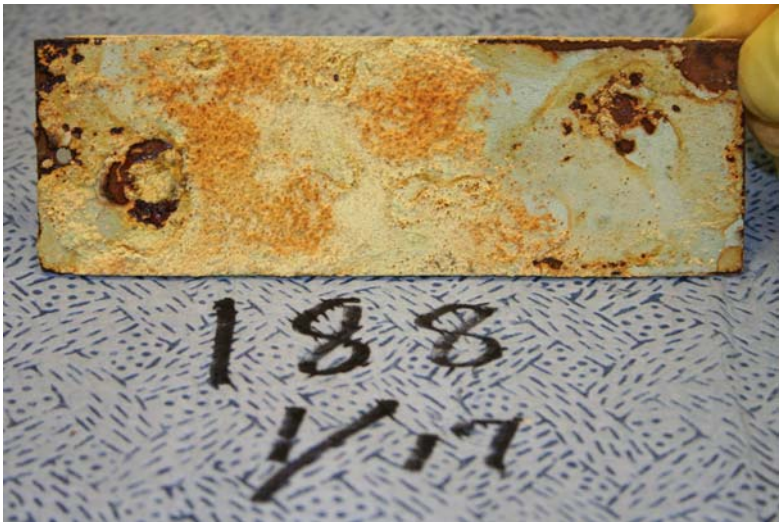

Figure 10. Post-test photo of horizontal plate from Test 2 (75°C, mixed).

Figure 11. Post-test photo of vertical coupons from Test 4 (50 °C, unmixed). Note goethite and humboldtine on first three coupons.

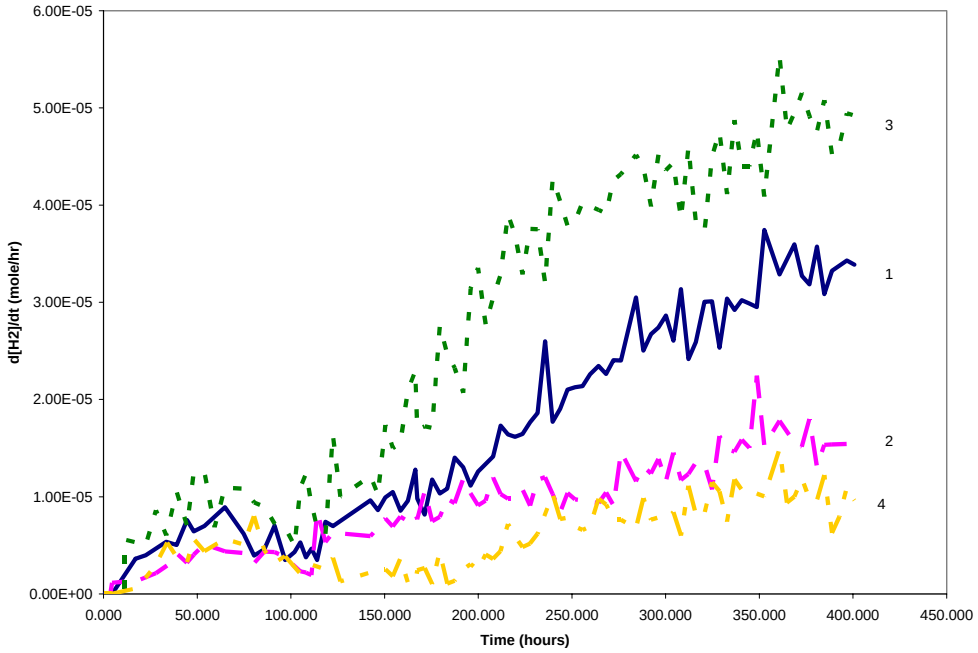

Figure 12. Hydrogen generation rate vs. times for radiation tests at 50 °C. Containers 1 and 3 were in the radiation source and 2 and 4 were outside.

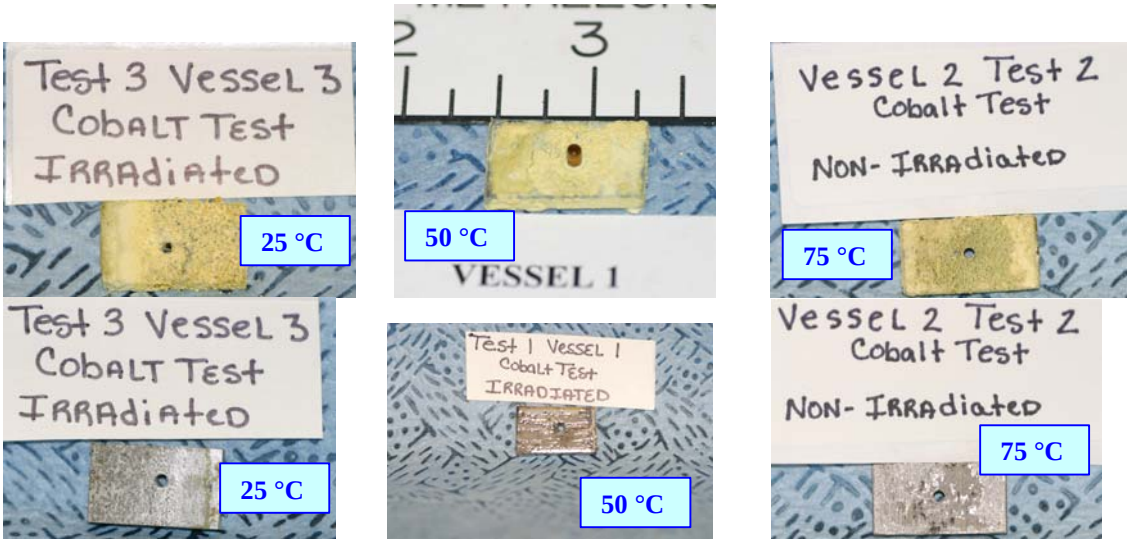

Figure 13. Representative coupons from irradiated corrosion testsTop row coupons were photographed at the completion of the test, while the bottom row coupons were photographed after the coupon was cleaned and prior to weighing.